Needle-free Injection of Hyaluronic Acid for Skin Remodeling via Modulation of Vimentin in a Mouse Model

Journal:	*International Journal of Dermatology*
Manuscript ID:	Draft
Manuscript Type:	Dermatologic Surgery
Date Submitted by the Author:	n/a
Complete List of Authors:	Kwon, Tae-Rin; Chung-Ang University College of Medicine, Department of Dermatology Jang, Ji-Hye; Amorepacific R&D center, DDS team Kwon, Min Kyung; Amorepacific R&D center, DDS team Oh, Chang Taek; Chung-Ang University College of Medicine, Department of Dermatology Shin, Dong Ha; Chung-Ang University College of Medicine, Department of Dermatology Choi, Eun Ja; Chung-Ang University College of Medicine, Department of Dermatology Hong, Hyuckki; Korea Electronics Technology Institute, Medical IT Research Center; Korea Electronics Technology Institute, Medical IT Convergence Research Center Choi, Yeonshik; Korea Electronics Technology Institute, Medical IT Convergence Research Center Kim, Beom Joon; Chung-Ang University, College of Medicine, Department of Dermatology; Bae, Joonho; Amorepacific R&D center, DDS team
Keywords:	collagen, cosmetic dermatology, biology

Needle-free Injection of Hyaluronic Acid for Skin Remodeling via Modulation of Vimentin in a Mouse Model

Tae-Rin Kwon[1, 2*], Ji-Hye Jang[3*], Min Kyung Kwon[3], Chang Taek Oh[1, 2], Dong Ha Shin[2], Eun Ja Choi[2], Hyuck ki Hong[4], Yeon Shik Choi[4], Beom Joon Kim[1,2], Joonho Bae[3†]

1Department of Medicine, Graduate School, Chung-Ang University, Seoul, Korea

2Department of Dermatology, Chung-Ang University College of Medicine, Seoul, Korea

3Medical Beauty Research Institute, Amorepacific Co., R&D Center, Yongin-si, Gyeonggi-do, Korea.

4Medical IT convergence Research center, Korea Electronics Technology Institute, Gyeonggi-do, Korea

** These authors contributed equally to this study.*

Running title: HA-Delivery System for Mouse Model

Keywords: Collagen, Cosmetic dermatology, Biology

Corresponding author: Joonho Bae, Ph.D, DDS Team, Medical Beauty Research Div., AmorePacific R&D Center 1920, Yonggu-Daero, Giheung-gu, Yongin-si, Gyeonggi-do, Korea, 446-729

E-mail: rachisis@amorepacific.com, Tel: 82-31-280-5940, Fax: 82-31-284-3995

ABSTRACT

Background The jet injector uses a pneumatically accelerated high-speed jet to penetrate the skin via a very small entry point in the epidermis and has demonstrated efficacy in clinical trials. However, despite its popularity its mechanisms of action are not yet fully defined and the technique has not been fully evaluated.

Aim We investigated the mechanism of action, efficacy, and safety of the pneumatic device using injection of hyaluronic acid (HA) solution into a mouse model.

Methods We evaluated the efficacy and safety of an INNOJECTOR™ pneumatic device that pneumatically accelerates a jet of HA solution under high pressure into the dermis of mouse skin. We examined the treatment effects using in vitro jet dispersion experiments, a skin hybrid model, photographic images, microscopy, and histologic analyses.

Results Use of the INNOJECTOR™ successfully increased dermal thickness and collagen synthesis in our mouse model. Jet dispersion experiments were performed using agarose gels and a polyacrylamide gel model to understand the dependence of jet penetration on jet power. The mechanisms by which pneumatic injection using HA solution exerts its effects may involve increased dermal thickening, triggering of a wound healing process, and activation of vimentin and collagen synthesis.

Conclusions Pneumatic injection of HA under high pressure provides a safe and effective method for improving the appearance of mouse skin. Our findings indicate that use of the INNOJECTOR™ may induce efficient collagen remodeling with subsequent marked dermal layer thickening by targeting vimentin.

INTRODUCTION

Skin aging is a complex biological process that is a consequence of both intrinsic and genetically programmed aging that occurs with time and extrinsic aging caused by environmental factors [1]. The dramatic increase in the aging population and the psychosocial impact of skin aging has created a demand for effective interventions [2]. Currently, various nonablative skin resurfacing techniques are being used to rejuvenate facial skin, including lasers and intense pulsed light (IPL) [3]. Several energy-based skin rejuvenation technologies, such as lasers [4], radiofrequency [5] or ultrasound [6], aim to trigger collagen remodeling in response to controlled thermal damage of the dermal skin layers. All of these modalities produce controlled thermal damage in the dermal layers of the skin that can lead to limited long-term effects after several months of treatment but usually lack any immediate effect [7].

Jet injection uses a high-speed stream of fluid to puncture the skin and deliver drugs to the dermal or subdermal region without the use of a needle [8, 9]. Recently, jet injectors have also been applied for gene and vaccine delivery [10, 11]; however, occasional pain and bruising limit the widespread use of jet injectors [12]. For skin rejuvenation, jet injection uses precise technology to accelerate and laterally disperse skin-enhancing hyaluronic acid (HA) particles via microtrauma using a pneumatic needle-free action. These particles enter the dermis to a controlled depth while leaving the surrounding tissue intact, and induce dermal microtrauma that mechanically stretches the fibroblasts, stimulating growth factors and inhibiting collagen breakdown [13]. Previous reports have demonstrated that Airgent™ triggers natural wound healing and augments collagen generation for enhanced effectiveness and long-lasting changes in the dermis [13; 14], but the exact mechanism by which this process of collagen generation is initiated remains unclear.

Vimentin is a marker of fibroblasts and myofibroblasts and a component of type III intermediate filaments [15]. Vimentin filaments in mesenchymal cells are involved in motility, maintenance of cell shape, and endurance of mechanical stress [16]. In particular, vimentin-

deficient mice exhibit delayed wound healing [17]. Thus, vimentin filaments play a role in wound healing and the development of tissue fibrosis.

The main aims of the current study were to evaluate the mechanisms of action, efficacy, and safety and of the INNOJECTOR™ pneumatic device in a mouse model. Our findings indicate that pneumatic injection of HA stabilizes collagen synthesis by targeting vimentin.

MATERIALS AND METHODS

Jet production

The needle-free microjet injection device INNOJECTOR™ (Provided by Amore Pacific, Korea) is a novel way to introduce various materials such as aesthetic medicines, HA, botolinum toxin, and placental extracts into the skin without pain and bleeding. The accelerated jet penetrates the epidermis through a tiny entry point. This device produces a high-velocity jet (up to 180 m/s) with a nozzle diameter of 0.1 mm that penetrates the skin and delivers medicines intradermally using a liquid propelled by compressed gasses (nozzle diameter 0.1 mm, max velocity 180 m/s). In this study, a solution of Bromocresol green dye (1% v/v) in deionized (DI) water was used as the jet fluid for in vitro assessment of penetration in gels. The liquid volume ejected in each jet was 0.15 ml and jets were ejected at a distance of 1 mm from 0.5, 1, 1.5% agarose gel or 20% polyacrylamide gels. For mouse studies, injection was performed by pneumatically accelerating a carrier fluid jet containing high-mass molecules of HA.

Animals and experimental design

Fifty female SKH-1 hairless mice (7 weeks old) were purchased from Central Laboratory Animal Inc. (Seoul, Korea), and assigned into 5 groups with 10 mice in each group. The animals were kept in a controlled environment with constant temperature and humidity and a

12-h light/dark cycle, and were fed a standard diet and given water ad libitum. Mice were given an anesthetic overdose of Zoletil (25 mg/kg, i.p.) before treatment of the dorsal skin areas with conventional needle injection or with an INNOJECTOR pneumatic device that delivered HA dermal filler (Haviscoplus INJ 10 mg/ml, Pacific Pharma, Korea) diluted in saline into the dermis via pneumatic needleless action. A solution of HA dermal filler (10% v/v) in saline was used as the jet fluid. The mice were followed for 14 days post-treatment before being humanely sacrificed. All procedures involving animals were conducted in accordance with the guidelines of the Institutional Animal Care and Use Committee of Chung Ang University in Korea (IRB Number: 13-0070).

Skin surface change

Morphologic changes in the dorsal skin surface after treatment were examined using a folliscope (LeedM, Seoul, Korea), a small handheld USB connection-based apparatus containing a high definition microscopic camera that is operated using a computer screen as an interface. We obtained photographs of the skin surface on days 0, 1, and 14.

Histologic examination

Skin samples of the areas treated by pneumatic needleless injection or conventional needle injection were taken immediately after measurement of skin thickness. The skin tissues were fixed with 4% paraformaldehyde (PFA) and embedded in paraffin. Subsequently, 5-μm thick sections were cut using a microtome, transferred to probe-on-plus slides (Fisher Scientific, Pittsburg, PA, USA), and stained with hematoxylin and eosin (H&E) to evaluate epidermal and dermal changes. Ten sections were assessed for each experimental group. Dermal thickness was measured from the dermal epidermal junction to the underlying subcutaneous tissue. The mean value was calculated and used as the final dermal thickness. Histopathologic

analysis of images taken under a microscope (BX51®, Olympus) was performed using computerized digital imaging micrometer software (Olympus Stream Modular Imaging Software®).

Picro-sirius red assay

Sections were stained with Sirius red (Sigma, Steinheim, Germany) at room temperature for 1 h. After staining, sections were hydrated through serial concentrations of ethanol, cleared with xylene, and mounted with neutral resin. Collagen types I and III were differentiated by polarization microscopy (PLM; Motic BA 300 POL, Richmond, BC, Canada) in which collagen type I showed as bright red and collagen type III as green.

Immunohistochemical analyses

Sections were stained using mouse monoclonal antibodies against collagen I (1:200, ab292, Abcam, Cambridge, MA, USA) and vimentin (1:500, ab92547, Abcam). Immunohistochemical analyses were performed with a high temperature antigen unmasking technique. In brief, the sections were heated in an unmasking solution (citrate buffer, pH 6.0), washed, and incubated with primary monoclonal antibodies at room temperature for 1 h followed by incubation with secondary antibodies (Envision Detection kit K5007, DAKO, Glostrup, Denmark). The reaction products were developed using 3,3′-diaminobenzidine, and the sections were rinsed and counterstained with hematoxylin to visualize the nuclei. The sections were dehydrated and covered with permount (Fisher Scientific, Fair Lawn, NJ, USA) and coverslips. Histologic changes were assessed by light microscopy.

Statistical analyses

Statistical comparisons between the treated and untreated groups were performed using one-

way ANOVA analyses followed by post-hoc Tukey for direct comparison. The results are expressed as mean ± standard deviation of at least three independent experiments, and P values of $p < 0.05$ *, $p < 0.01$ **, and $p < 0.001$ *** were considered statistically significant.

RESULTS

Determination of penetration depth and morphologic features of the injection site

To evaluate the effects of the INNOJECTOR™ pneumatic device in an *in vitro* assay, we measured the penetration depths of 1% bromocresol green solution (0.15 ml/ 2.52*10^5Mpa) injected into agarose gels or polyacrylamide gels. In this experiment we focused on single injection sites. Agarose gels with concentrations of 0.5, 1.0, and 1.5% and 20% polyacrylamide gels were injected as described in Materials and Methods. The penetration depth and morphology of the upper layer of the gel was determined by examination using a folliscope. Jet penetration into various gel types produced a cylindrical hole starting at the point of jet impact, followed by circular dispersion of fluid in the gels (Fig. 1A, B).

The depth of penetration was 8.85 ± 1.65 mm for 0.5% agarose gels, 6.95 ± 1.05 mm for 1% agarose gels, 5.65 ± 0.29 mm for 1.5% agarose gels, and 2.35 ± 0.26 mm for 20% polyacrylamide gels. Thus, penetration of 1% bromocresol green solution decreased linearly with increasing hardness (Fig. 1C). Physical application of the INNOJECTOR™ pneumatic device provided reproducible delivery of the injected material to the desired target site in a pressure-dependent manner. We next investigated changes in mouse skin tissue in the upper layers of the agarose gel. The average penetration of mouse skin tissue in the upper layers of the 1% agarose gel at the 2.52*10^5Mpa level was 4.35 ± 0.56 mm (Fig. 2A).

An erosion hole, as determined by increased size and height of the mouse skin, was observed immediately after jet injector application using Visioscan 98® (2.52*10^5Mpa-

induced site, blue color; 2.88*10^5MPa-induced site, red and yellow color; Figure 2B). The 3D images showed higher and brighter green bars with increasing pulse energy, clearly indicating that increasing the pulse energy generated microholes with greater depth. Therefore the jet penetration depth in skin seems to be dependent on jet power.

Together, our results suggest that the INNOJECTOR™ pneumatic device has comparable effects in skin as in various type gels, resulting in visible dispersion of fluid. In particular, the effect of jet velocity and nozzle diameter on the depth of the erosion hole formed was very similar in gels and in skin.

Histologic evaluation of mouse skin after needle-free injection versus conventional needle injection

Mouse skin obtained 14 days post-treatment was analyzed for skin surface changes and detection of microholes using a folliscope. We examined dermis outside of the focal region of the single injection site in the INNOJECTOR™ groups (Fig. 3).

As shown in Fig. 4A, H&E-stained sections showed marked full-thickness regeneration with a thick and well-organized dermis after needle-free injection comparable to that observed after conventional needle injection, which does not induce the wound generation and healing process. Full-thickness epidermal-dermal regeneration that completely covered the wound area was observed. Moreover, the dermis became even and the thickness increased markedly in the needle-free injection groups, comparable to conventional needle injection (Fig. 4C). Next, we investigated skin changes with picro-sirius red staining. At day 14, a marked increase in collagen fibers and fibroblasts in the hypodermis was detected after needle-free injection, compared with the controls (Fig. 4B). With the activation of fibroblasts the number of collagen fibers began to increase, changing from disorganized collagen with reduced affinity for the stain to formation of new collagen with an improvement in the organization of

collagen fibrils. Based on these findings, we concluded that the INNOJECTOR™ pneumatic device effectively induced collagen synthesis and increased skin thickness in the mouse model.

Activation of vimentin by needle-free injection

To evaluate the mechanism underlying the activation of collagen synthesis in this mouse model we performed immunohistochemistry on mouse skin specimens using antibodies specific to collagen I or vimentin. Previous reports have suggested that vimentin is one of the major components of the cytoskeleton structure [18]; however, the effects of direct activation of vimentin on collagen synthesis are still not fully understood. In the mouse model we observed a remarkable increase in vimentin protein expression in fibroblasts and myofibroblasts of the dermis from day 7 post-treatment with filler in the needle-free injection group compared with the conventional needle injection group (Fig. 5). In particular, vimentin staining revealed greatly increased numbers of filler granules around the injection site in the dermis. Overall, our findings suggest that use of the INNOJECTOR™ pneumatic device for wrinkle reduction may affect collagen synthesis through the activation of vimentin in fibroblasts and myofibroblasts.

DISCUSSION

Jet injection is a needle-free delivery method in which a high-speed stream of fluid impacts the skin [19]. Previous studies have shown the effectiveness of pneumatic devices for the treatment of acne scars [20] and depressed scars of the forehead secondary to herpes zoster infection using subdermal minimal surgery technology [21]. Consequently, a number of jet injectors are commercially available, even though the biologic mechanisms of jet injection are still poorly understood.

We first used a newly developed INNOJECTOR™ pneumatic device to inject gels and an *in vitro* skin-gel hybrid model. As shown in Figures 1 and 2, the INNOJECTOR™ pneumatic device showed similar erosion dependence in skin as in various type gels. Morphologic analysis demonstrated increased size and height of the mouse skin immediately after application of the jet injector (Fig. 2). These results indicate that the INNOJECTOR™ pneumatic device exhibits efficacy and safety as a skin remodeling device.

We next evaluated the efficacy of jet injectors using a mouse model. Our data suggested that jet injectors modulate dermal collagen metabolism and induce morphologic changes (Fig. 3). The INNOJECTOR™ pneumatic device delivered diluted HA dermal filler solution into the dermis via pneumatic needleless action. Recent clinical studies have shown that microtrauma to dermal cells triggers natural wound healing processes and augments collagen generation for long-term effectiveness and long lasting changes in the dermis [13]. However, the HA delivery system has not yet been studied in a mouse model.

Histologic analysis demonstrated increases in skin thickness and collagen fibers in the dermis after needle-free injection (Fig. 4A and B). These results indicate that needle-free injection exerts anti-wrinkle effects in the mouse model. In particular, picro-sirius red staining revealed an increase in not only type I collagen, but also type III collagen, at 14 days after needle-free injection.

HA attracts water molecules, producing immediate thickening and hydration in the dermis and consequently a visible aesthetic improvement [22]. Moreover, our data suggest possible induction of a wound healing response by the mechanical microtrauma of the pneumatic injection. Thus, collagen content in the dermis is determined by the balance between the number of dermal fibroblasts, collagen production, and collagen degradation.

Vimentin has emerged as an organizer of a number of critical proteins involved in cell attachment, migration, and signaling. Recent studies have revealed several key functions for

vimentin [23], [24], [25]. We performed immunohistochemistry to evaluate the mechanisms underlying the increased dermal thickness and induction of collagen synthesis in the mouse model after needle-free injection of HA filler. Our results indicated that these effects were probably the result of increased fibroblast proliferation via activation of vimentin (Fig. 5). These findings suggest that vimentin may play a key role in the signal transduction pathways that contribute to organization of collagen fibrils. However, our present study followed subjects for only 14 days after treatment and further long-term data will be required to determine the lasting effects of pneumatic treatment. Additionally, future studies are needed to determine the optimum treatment regimen.

In this study we used pneumatic needle-free injection of a fluid with diluted high-mass HA molecules to deliver HA dermal filler solution into the dermis. The resultant wound healing process stimulates growth factors and promotes the formation of new collagen fibers, resulting in skin remodeling [26]. Our results suggest that the INNOJECTOR™ pneumatic device effectively induced collagen synthesis via activation of vimentin. The biological performance of this needle-free injection system in the mouse skin model might provide valuable information on the feasibility of using devices already in clinical phases of product development for skin rejuvenation in humans.

Acknowledgements

This work was supported by the Infrastructure program for new-growth Industries (10044186, Development of Smart Beauty Devices Technology and Establishment of Commercialization Support Center), and funded by the Ministry of Trade, Industry & Energy (MI, Korea)

FIGURE LEGENDS

Fig. 1. Evaluation of *in vitro* dye injection and penetration depth. (a) Typical jet penetration shapes after injection (0.15 ml / 2.52*10^5Mpa) of 1% bromocresol green into 0.5%, 1%, 1.5% agarose gel and 20% polyacrylamide gels using an INNOJECTOR™ pneumatic device (Provided by Amore Pacific Inc). (b) Transverse slices of the gel visualized using a folliscope verify the presence of a hole in the gel. (c) Penetration depth at the end of the erosion period captured by photography and from visual observation post-injection. Data are shown for injections of 0.15 ml fluid traveling at an average speed of 180 m/s from a 0.1-mm diameter nozzle into 0.5%, 1%, 1.5% agarose gel and 20% polyacrylamide gels. Data are expressed as mean ± standard deviation (N=3). *P < 0.05, **P < 0.01, ***P < 0.001 compared to Normal.

Fig. 2. Injection of skin hybrid model. (a) Typical jet penetration shapes after injection into 0.5%, 1%, 1.5% agarose gels, 20% polyacrylamide gels containing a mouse dorsal skin sample in the outer layer (Red arrow). (b) Transverse slices of the gel visualized using a folliscope confirm the presence of a hole in the mouse skin samples. VC98 images were used to assess changes in depth of the mouse skin surface.

Fig. 3. *In vivo* changes in the skin surface. Effects of the INNOJECTOR™ pneumatic device on clinical and morphologic features of the injection site in hairless mice. Progression of skin surface changes for the different intervention groups was analyzed throughout a 14-day observation period. Changes in microtrauma morphology were evaluated using images taken with a folliscope (×30).

Fig. 4. Effects of pneumatic device application on skin thickness and collagen synthesis in mouse skin. Typical photographs of histology for each panel. The effect of the

INNOJECTOR™ pneumatic device on mouse dorsal skin was analyzed by staining with hematoxylin-eosin (H&E) (a) and picro-sirius red (PSR) (b). (c) Dermal thickness was measured from the dermal-epidermal junction to the underlying subcutaneous tissue. Ten sections were assessed in each experimental group. The mean value was calculated and used as the final dermal thickness. Data are expressed as mean ± standard deviation (N=10). Original magnification, ×100.

Fig. 5. Immunohistochemical identification of vimentin-positive cells in mouse skin tissue sections. Skin biopsies were taken 14 days after injection and analyzed by immunohistochemistry. The collagen type I-positive and vimentin-positive areas were stained by 3,3′-diaminobenzidine with a hematoxylin counterstain to visualize the nuclei. Original magnification, ×100, ×200.

REFERENCES

1 J. Uitto, E. F. Bernstein. Molecular mechanisms of cutaneous aging: connective tissue alterations in the dermis. *J Investig Dermatol Symp Proc* 1998; 3: 41-44.

2 J. L. McCullough, K. M. Kelly. Prevention and treatment of skin aging. *Ann N Y Acad Sci* 2006; 1067: 323-331.

3 A. L. Tajirian, D. J. Goldberg. Fractional ablative laser skin resurfacing: a review. *J Cosmet Laser Ther* 2011; 13: 262-264.

4 J. Lipozencic, Z. Bukvic Mokos. Dermatologic lasers in the treatment of aging skin. *Acta Dermatovenerol Croat* 2010; 18: 176-180.

5 A. Wirtzer. Nonablative radiofrequency for skin rejuvenation. *Dermatol Surg* 2010; 36: 2083-2084.

6 K. Minkis, M. Alam. Ultrasound skin tightening. *Dermatol Clin* 2014; 32: 71-77.

7 E. P. Tierney, D. J. Kouba, C. W. Hanke. Review of fractional photothermolysis: treatment indications and efficacy. *Dermatol Surg* 2009; 35: 1445-1461.

8 S. Mitragotri. Current status and future prospects of needle-free liquid jet injectors. *Nat Rev Drug Discov* 2006; 5: 543-548.

9 J. Baxter, S. Mitragotri. Needle-free liquid jet injections: mechanisms and applications. *Expert Rev Med Devices* 2006; 3: 565-574.

10 Y. Taniyama, J. Azuma, Y. Kunugiza, K. Iekushi, H. Rakugi, R. Morishita. Therapeutic option of plasmid-DNA based gene transfer. *Curr Top Med Chem* 2012; 12: 1630-1637.

11 M. A. Kendall. Needle-free vaccine injection. *Handb Exp Pharmacol* 2010: 193-219.

12 S. Mitragotri. Devices for overcoming biological barriers: the use of physical forces to disrupt the barriers. *Adv Drug Deliv Rev* 2013; 65: 100-103.

13 A. Levenberg, S. Halachmi, A. Arad-Cohen, D. Ad-El, D. Cassuto, M. Lapidoth. Clinical results of skin remodeling using a novel pneumatic technology. *Int J Dermatol* 2010; 49: 1432-1439.

14 K. F. Kobus, T. Dydymski. Quantitative dermal measurements following treatment with AirGent. *Aesthet Surg J* 2010; 30: 725-729.

15 E. Fuchs, K. Weber. Intermediate filaments: structure, dynamics, function, and disease. *Annu Rev Biochem* 1994; 63: 345-382.

16 L. Chang, Y. Shav-Tal, T. Trcek, R. H. Singer, R. D. Goldman. Assembling an intermediate filament network by dynamic cotranslation. *J Cell Biol* 2006; 172: 747-758.

17 P. Bargagna-Mohan, R. R. Paranthan, A. Hamza *et al.* Corneal antifibrotic switch identified in genetic and pharmacological deficiency of vimentin. *J Biol Chem* 2012; 287: 989-1006.

18 M. Guo, A. J. Ehrlicher, S. Mahammad *et al.* The role of vimentin intermediate filaments in cortical and cytoplasmic mechanics. *Biophys J* 2013; 105: 1562-1568.

19 M. A. Logomasini, R. R. Stout, R. Marcinkoski. Jet injection devices for the needle-free administration of compounds, vaccines, and other agents. *Int J Pharm Compd* 2013; 17: 270-280.

20 J. W. Lee, B. J. Kim, M. N. Kim, C. K. Lee. Treatment of acne scars using subdermal minimal surgery technology. *Dermatol Surg* 2010; 36: 1281-1287.

21 B. J. Kim, K. H. Yoo, M. N. Kim. Successful treatment of depressed scars of the forehead secondary to herpes zoster using subdermal minimal surgery technology. *Dermatol Surg* 2009; 35: 1439-1440.

22 T. V. Anilkumar, J. Muhamed, A. Jose, A. Jyothi, P. V. Mohanan, L. K. Krishnan. Advantages of hyaluronic acid as a component of fibrin sheet for care of acute wound. *Biologicals* 2011; 39: 81-88.

23 A. S. Menko, B. M. Bleaken, A. A. Libowitz, L. Zhang, M. A. Stepp, J. L. Walker. A central role for vimentin in regulating repair function during healing of the lens epithelium. *Mol Biol Cell* 2014; 25: 776-790.

24 M. Murakami, K. Imabayashi, A. Watanabe *et al.* Identification of novel function of vimentin for quality standard for regenerated pulp tissue. *J Endod* 2012; 38: 920-926.

25 O. Jungmann, K. Nikolovska, C. Stock *et al.* The dermatan sulfate proteoglycan decorin modulates alpha2beta1 integrin and the vimentin intermediate filament system during collagen synthesis. *PLoS One* 2012; 7: e50809.

26 P. Martin. Wound healing--aiming for perfect skin regeneration. *Science* 1997; 276: 75-81.

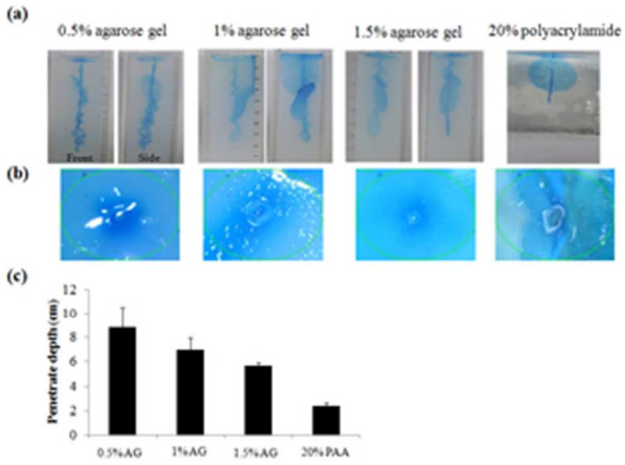

Fig. 1. Evaluation of in vitro dye injection and penetration depth. (a) Typical jet penetration shapes after injection (0.15 ml / 2.52*10^5Mpa) of 1% bromocresol green into 0.5%, 1%, 1.5% agarose gel and 20% polyacrylamide gels using an INNOJECTORTM pneumatic device (Provided by Amore Pacific Inc). (b) Transverse slices of the gel visualized using a folliscope verify the presence of a hole in the gel. (c) Penetration depth at the end of the erosion period captured by photography and from visual observation post-injection. Data are shown for injections of 0.15 ml fluid traveling at an average speed of 180 m/s from a 0.1-mm diameter nozzle into 0.5%, 1%, 1.5% agarose gel and 20% polyacrylamide gels. Data are expressed as mean ± standard deviation (N=3). *P < 0.05, **P < 0.01, ***P < 0.001 compared to Normal.
26x20mm (300 x 300 DPI)

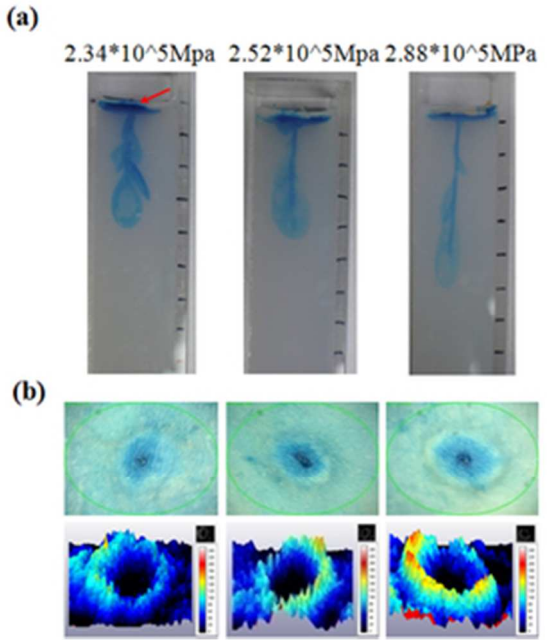

Fig. 2. Injection of skin hybrid model. (a) Typical jet penetration shapes after injection into 0.5%, 1%, 1.5% agarose gels, 20% polyacrylamide gels containing a mouse dorsal skin sample in the outer layer (Red arrow). (b) Transverse slices of the gel visualized using a folliscope confirm the presence of a hole in the mouse skin samples. VC98 images were used to assess changes in depth of the mouse skin surface.
23x27mm (300 x 300 DPI)

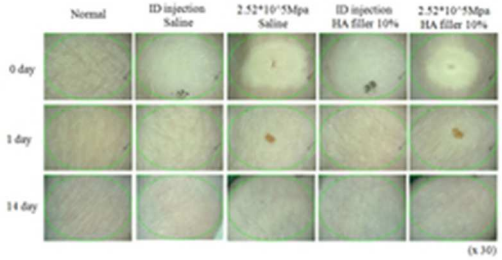

Fig. 3. In vivo changes in the skin surface. Effects of the INNOJECTORTM pneumatic device on clinical and morphologic features of the injection site in hairless mice. Progression of skin surface changes for the different intervention groups was analyzed throughout a 14-day observation period. Changes in microtrauma morphology were evaluated using images taken with a folliscope (×30).
21x11mm (300 x 300 DPI)

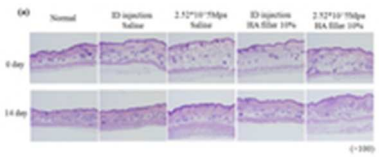

Fig. 4. Effects of pneumatic device application on skin thickness and collagen synthesis in mouse skin. Typical photographs of histology for each panel. The effect of the INNOJECTORTM pneumatic device on mouse dorsal skin was analyzed by staining with hematoxylin-eosin (H&E) (a) and picro-sirius red (PSR) (b). (c) Dermal thickness was measured from the dermal-epidermal junction to the underlying subcutaneous tissue. Ten sections were assessed in each experimental group. The mean value was calculated and used as the final dermal thickness. Data are expressed as mean ± standard deviation (N=10). Original magnification, ×100.
16x6mm (300 x 300 DPI)

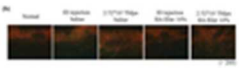

Fig. 4. Effects of pneumatic device application on skin thickness and collagen synthesis in mouse skin. Typical photographs of histology for each panel. The effect of the INNOJECTORTM pneumatic device on mouse dorsal skin was analyzed by staining with hematoxylin-eosin (H&E) (a) and picro-sirius red (PSR) (b). 10x2mm (300 x 300 DPI)

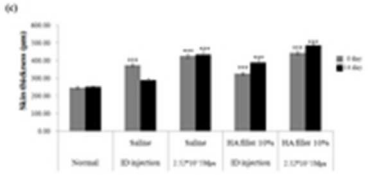

Fig. 4. Effects of pneumatic device application on skin thickness and collagen synthesis in mouse skin. Typical photographs of histology for each panel. The effect of the INNOJECTORTM pneumatic device on mouse dorsal skin was analyzed by staining with hematoxylin-eosin (H&E) (a) and picro-sirius red (PSR) (b). (c) Dermal thickness was measured from the dermal-epidermal junction to the underlying subcutaneous tissue. Ten sections were assessed in each experimental group. The mean value was calculated and used as the final dermal thickness. Data are expressed as mean ± standard deviation (N=10). Original magnification, ×100.
17x7mm (300 x 300 DPI)

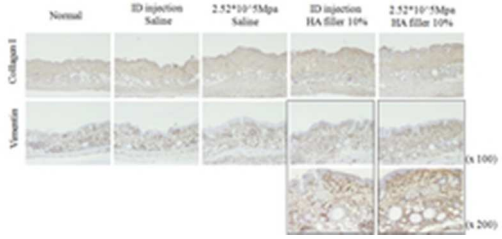

Fig. 5. Immunohistochemical identification of vimentin-positive cells in mouse skin tissue sections. Skin biopsies were taken 14 days after injection and analyzed by immunohistochemistry. The collagen type I-positive and vimentin-positive areas were stained by 3,3′-diaminobenzidine with a hematoxylin counterstain to visualize the nuclei. Original magnification, ×100, ×200.
21x10mm (300 x 300 DPI)